Development 133, 3797-3804 (2006) doi:10.1242/dev.02550

Arteries define the position of the thyroid gland during its developmental relocalisation

Burkhard Alt[1,*], Osama A. Elsalini[1,*], Pamela Schrumpf[2,*], Nele Haufs[2], Nathan D. Lawson[3], Georg C. Schwabe[4], Stefan Mundlos[4], Annette Grüters[2], Heiko Krude[2,†] and Klaus B. Rohr[1,†]

During vertebrate development, the thyroid gland undergoes a unique relocalisation from its site of induction to a distant species-specific position in the cervical mesenchyme. We have analysed thyroid morphogenesis in wild-type and mutant zebrafish and mice, and find that localisation of growing thyroid tissue along the anteroposterior axis in zebrafish is linked to the development of the ventral aorta. In grafting experiments, ectopic vascular cells influence the localisation of thyroid tissue cell non-autonomously, showing that vessels provide guidance cues in zebrafish thyroid morphogenesis. In mouse thyroid development, the midline primordium bifurcates and two lobes relocalise cranially along the bilateral pair of carotid arteries. In hedgehog-deficient mice, thyroid tissue always develops along the ectopically and asymmetrically positioned carotid arteries, suggesting that, in mice (as in zebrafish), co-developing major arteries define the position of the thyroid. The similarity between zebrafish and mouse mutant phenotypes further indicates that thyroid relocalisation involves two morphogenetic phases, and that variation in the second phase accounts for species-specific differences in thyroid morphology. Moreover, the involvement of vessels in thyroid relocalisation sheds new light on the interpretation of congenital thyroid defects in humans.

KEY WORDS: Thyroid, Zebrafish, Mouse, Arteries, Vegf, Scl, Hedgehog

INTRODUCTION

The vertebrate body plan is essentially established during early development. However, the final position and shape of organs also depends on later events in morphogenesis. This is particularly evident for endoderm-derived organs, such as the thyroid gland, lung, pancreas and liver. The primordia of these organs bud off from different positions of the primitive gut and then undergo major morphogenetic alterations, such as branching and extension of the lung and lateralisation of the liver primordia. Relocalisation of an organ primordium is particularly evident in thyroid development. Its primordium evaginates from the pharyngeal epithelium after induction, to adopt a distant, species-specific position in the cervical mesenchyme. This relocalisation of the thyroid primordium is often called 'migration'. We here avoid this term, as active movement of thyroid primordial cells has not been proven, and the molecular mechanisms of thyroid relocalisation are largely elusive. The transcription factor Foxe1 is cell autonomously required for proper relocalisation, as shown in mouse embryos and humans with congenital hypothyroidism (Castanet et al., 2002; Dathan et al., 2002). However, the morphogenetic forces defining the position of organ tissue during the relocalisation process are unknown.

The disruption of morphogenetic events defining position and shape of organs can account for congenital malformations and diseases in humans. The thyroid is particularly prone to morphogenetic variability. Usually present as a bilobed gland in humans, the thyroid develops as a unilateral gland at a frequency of one in 2000 individuals (Maiorana et al., 2003). Furthermore, the whole or part of the thyroid tends to develop ectopically, either at positions reminiscent of the relocalisation path or at apparently unrelated positions, for example embedded into heart tissue close to the outflow tract (Casanova et al., 2000). Proper organ function usually depends on normal tissue localisation with respect to adjacent structures during development. Therefore, ectopic localisation of the thyroid gland is often associated with compromised endocrine function, resulting in congenital hypothyroidism (De Felice and Di Lauro, 2004).

Owing to its accessibility for embryonic manipulation, the zebrafish thyroid is an excellent model with which to identify structures required for proper thyroid localisation. As far as investigated, molecules involved in thyroid development are essentially conserved between zebrafish and mammals (Elsalini et al., 2003; Wendl et al., 2002). In zebrafish, rapid development might explain a slightly different timing in thyroid differentiation (Elsalini et al., 2003). More striking differences between species exist with respect to the final position and shape of the gland. Although in all vertebrates investigated the primordium relocalises after evagination from the pharyngeal epithelium, the gland eventually adopts different shapes (Gorbman and Bern, 1962). In zebrafish, the initially small globular thyroid grows massively along the anteroposterior axis in the hypopharyngeal area, expanding into a long strand of tissue (Alt et al., 2006). In mouse and humans, the gland adopts its characteristic bilobed shape in front of the trachea.

In the present study, we investigate how thyroid tissue is positioned during relocalisation. Using zebrafish, we show that ectopic vascular cells are sufficient to mislocate thyroid tissue in a non-cell autonomous manner during growth. Based on this finding and on analysis of zebrafish mutants, we conclude that an adjacent vessel, the ventral aorta, determines thyroid tissue localisation. In the derived circulation of mammals, a vessel homologous to the ventral aorta does not persist. By investigating normal and mutant mouse embryos, we identify the carotid arteries as candidates for vessels that have assumed a comparable role in mammalian thyroid morphogenesis.

[1]Institute for Developmental Biology, University of Cologne, Gyrhofstrasse 17, 50923 Köln, Germany. [2]Institute for Paediatric Endocrinology, Charite University Hospital, Humboldt-University, Berlin, Germany. [3]University of Massachusetts Medical School, 364 Plantation Street, Worcester, MA 01605, USA. [4]Max Planck Institute for Molecular Genetics, Berlin, Germany.

*These authors contributed equally to the work
†Authors for correspondence [e-mail: heiko.krude@charite.de (mouse); klaus.rohr@uni-koeln.de (zebrafish)]

Accepted 26 July 2006

MATERIALS AND METHODS

Animals

Zebrafish work was carried out according to standard procedures and staging in hours post fertilisation (hpf) refers to development at 28.5 to 29°C. The term 'larva' is used in the text for fry that have hatched from the chorion and generally refers to an age older than 72 hpf. The mutant zebrafish line *kdr*^{y17} (Covassin et al., 2006) is allelic to the *kdr* (*flk1*) lines described previously (Habeck et al., 2002) and develops heart oedema owing to compromised circulation or other specific defects at stages older than 40 hours, so that determination of mutant phenotypes was possible based on morphology. Homozygous *cloche* mutant embryos (*clo*^{s5}) (Stainier et al., 1995) were also identified before fixation according to their phenotype at 24 hpf. Phenotypic details described in this study were always evident in all homozygous specimens (more than 10 in each experiment).

For analysis of *short digits* (*Dsh/Dsh*) (Niedermaier et al., 2005) and *Xt*^{J}/*Xt*^{J} mutant mouse embryos (Persson et al., 2002) timed matings of mutants were generated. The homozygous phenotypes are distinguishable from wild type owing to severe morphological defects, and in the case of *Dsh-Xt*^{J} matings we determined the genotype by PCR from extra-embryonic membranes (primer information available upon request).

Preparation of specimens

In situ hybridisation on zebrafish was carried out according to standard procedures, using *nk2.1a* (Rohr and Concha, 2000) as molecular marker for the thyroid primordium. Whole-mount immunohistochemistry with antibodies against thyroid hormone (T4) or thyroglobulin (TG) in whole-mount zebrafish larvae was performed as described elsewhere (Elsalini and Rohr, 2003).

For histological analysis, paraffin embedded mouse embryos were sectioned and stained with Haematoxylin-Eosin according to standard protocols. Three-dimensional images were reconstructed using every fifth section with the program SURFdriver 4.0, available at http://www.surfdriver.com. For immunohistochemistry on mouse sections, we used a Nkx2.1/Ttf-1 specific antibody generated against rat recombinant antigen (DAKO, Carpenteria, USA). Zebrafish embryos were embedded in Durcupan and sectioned. Diameters of the thyroid were measured using Discus software on a DMRA2 compound microscope (Leica).

Embryonic manipulation

Synthetic mRNA was produced using the message machine kit (Ambion) and approximately 25 pg *scl* mRNA and 25 pg *lmo2* mRNA were injected into one cell stage embryos. As a control, we injected synthetic *gfp* mRNA at same concentrations. As lineage tracer for grafting experiments, we injected biotin-dextran (10.000 MW, 5 mg/ml; Invitrogen) together with synthetic mRNA and detected biotin-labelled donor-derived cells after in situ hybridisation using the ABC kit (Vector Laboratories). Injection and grafting experiments were repeated at least twice. At least 50 embryos were analysed for each mRNA injection experiment.

Morpholino RNA targeted against *vegf* (vegf-A-3) (Nasevicius et al., 2000), an *scl* splice morpholino (Patterson et al., 2005), a *tnnt2* morpholino (Sehnert et al., 2002) and an unspecific control morpholino were purchased (Gene Tools), and dissolved as recommended by the provider. Morpholinos were always injected into one cell stage embryos. At least 50 morphants were analysed for each experiment. Sections were made from five specimens or more in each experiment. All phenotypes described were consistently found in over 70% of morphants, with the rest showing milder defects or wild-type appearance.

RESULTS

The zebrafish thyroid primordium starts to develop at the outflow tract of the heart, which directly leads into the first primordial branch of pharyngeal arteries (Fig. 1A). From about 40 hours post fertilisation (hpf), the globular primordium expands along the anteroposterior (AP) axis into a strand of follicular tissue, thereby always remaining restricted to the midline (Fig. 1B-F). Close examination reveals that thyroid tissue expands in close contact to the growing ventral aorta (Fig. 1E-G). This major artery connects the heart to the branchial arteries that arise pairwise and sequentially, so that by 120 hpf a full set of five pairs of branchial arteries has formed (Isogai et al., 2001). The close association of thyroid and ventral aorta during development prompted us to investigate a possible relationship between both tissues.

Disturbed pharyngeal vessel architecture coincides with thyroid defects in zebrafish mutants

The mechanisms of ventral aorta and branchial artery development are largely unknown, so we first identified zebrafish embryos with disrupted pharyngeal vasculogenesis. The transcription factor Scl (also known as Tal1) is required for haematopoiesis (Gering et al., 1998; Liao et al., 1998), and endothelial (Liao et al., 1998) and dorsal aorta development (Patterson et al., 2005) in zebrafish embryos. Correspondingly, Scl is expressed in haematopoietic and

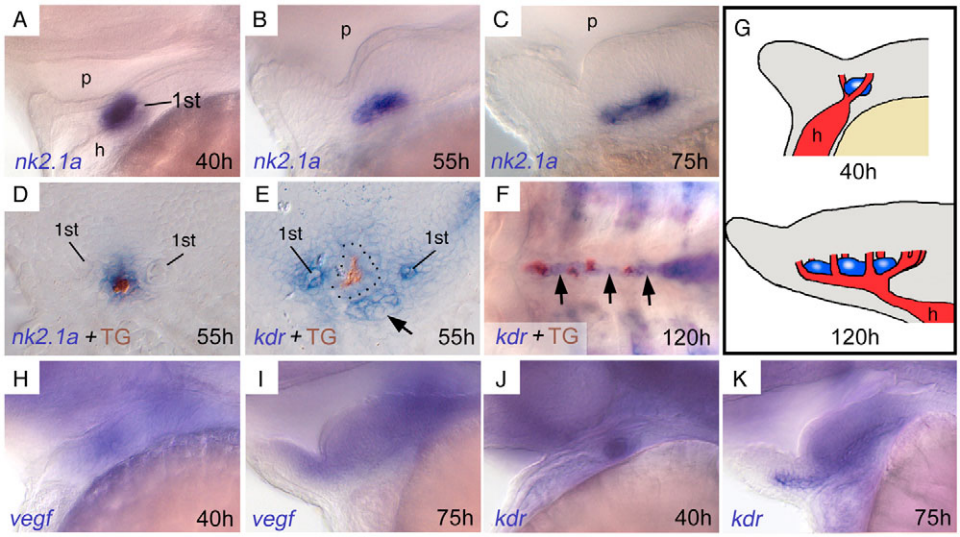

Fig. 1. The thyroid develops adjacent to the growing ventral aorta in zebrafish embryos. (**A-C**) Expression of the thyroid marker *nk2.1a* (blue) shows primordial expansion along the AP axis around 55 hpf. Lateral views, anterior towards the left. (**D**) An antibody against thyroglobulin (TG) visualises the lumen of thyroid follicles (brown), surrounded by follicular cells (blue). (**E**) The endothelial marker *kdr* is expressed in pharyngeal vessels around the thyroid (lumen brown, broken line around follicle cells), here showing the anterior tip of the ventral aorta on the level of the heart (arrow) and the first pair of branchial arteries (1st). (**F**) Throughout further development, thyroid tissue (follicles in brown) grows along the ventral aorta (arrows). Ventral view, anterior towards the left. (**G**) Schematic drawing summarising thyroid and vessel development. (**H**,**I**) *vegf* is diffusely expressed in the ventral pharyngeal area during ventral aorta development. Lateral views, anterior towards the left. (**J**,**K**) *kdr* is diffusely expressed in ventral aorta and surrounding mesenchyme (see also E). Lateral views, anterior towards the left. 1st, first pair of branchial arteries. h, heart; p, pharynx.

endothelial tissue, as well as in a few cells in the central nervous system (Jin et al., 2006). The vascular endothelial growth factor (Vegf) pathway plays crucial roles in vertebrate haematopoiesis and vasculogenesis (Ferrara, 2004). In zebrafish, Kdr (previously known as Flk1) is an endothelial cell specific Vegf receptor required for vasculogenesis (Covassin et al., 2006; Habeck et al., 2002), and *vegf* and *kdr* are also expressed in and around the nascent and growing ventral aorta (Fig. 1E,F,H-K). As expected from data regarding trunk vasculogenesis (Patterson et al., 2005), reduction of Scl or Vegf (using *scl* and *vegf* morpholinos) (Lawson et al., 2002; Nasevicius et al., 2000; Patterson et al., 2005), or absence of Kdr in kdr^{y17} mutant embryos (Habeck et al., 2002), dramatically interferes with pharyngeal vessel formation (Fig. 2A-D). Analysis of the endothelial marker *tie1* in the three deficiency backgrounds indicates that here the ventral aorta fails to form properly. Instead, a mis-shaped domain of *tie1* expression surrounds the outflow tract of the heart, often expanding laterally, but not along the AP axis, into one pair of irregular branches. Thus, Scl and the Vegf pathway are required for normal development and expansion of the ventral aorta along the AP axis.

We then analysed whether altered pharyngeal vessel architecture affects thyroid morphology. In the abovementioned three genetic backgrounds with compromised Scl activity or Vegf signalling, the thyroid starts to develop from a normally induced midline primordium at around 26 hpf (normally shaped and sized domain of *nk2.1a* expression, data not shown). However, during subsequent growth, the thyroid fails to elongate from its initial position at the cardiac outflow tract along the AP axis (Fig. 2E-H). Instead, thyroid tissue is not limited to the midline and often expands laterally in irregular fashion, always adjacent to or embedded into ectopic *tie1* expression (Fig. 2I-L). Correspondingly, follicles do not align along the pharyngeal midline during larval growth, and instead form an irregular group around the cardiac outflow tract (Fig. 2M-P). These data strongly suggest that thyroid morphogenesis is linked to pharyngeal vessel development.

To test whether compromised blood circulation evident in all of these deficiency backgrounds causes indirectly thyroid abnormalities, we targeted the *tnnt2* gene by morpholino knock down. *tnnt2* encodes the thin-filament contractile protein cardiac troponin T, and corresponding morphants lack heart beat and blood circulation (Sehnert et al., 2002). In these morphants, the thyroid is normal at 55 hpf (n=64, data not shown), showing that specific disruption of circulation does not account for morphological defects of the thyroid. Thus, it is rather vessel patterning that appears to be correlated to thyroid morphology. As the ventral aorta is the only vessel adjacent to the thyroid in wild type, it can be assumed that this is the artery that guides follicular growth along the midline. However, the thyroid phenotype in *scl* morphants could also be due to low level *scl* expression in thyroid tissue itself. Furthermore, *kdr* and *vegf* are broadly expressed around vessels (Fig. 1E,H-K), probably including thyroid cells, and therefore might act in parallel both in vascular cells and in thyroid cells. Thus, we asked whether ectopic endothelial cells are able to change thyroid morphology cell non-autonomously, as this would prove a direct interaction between vessels and thyroid.

Ectopic endothelial cells can influence thyroid morphology non-cell autonomously

To develop an assay in which cells are forced to adopt endothelial fate, we used an approach involving Scl and Lmo2, a transcription factor specifically required for haematopoiesis and angiogenesis (Yamada et al., 2000; Yamada et al., 1998). Co-injection of *scl* and *lmo2* mRNA induces ectopic expression of the endothelial marker *fli1* throughout the head mesenchyme of zebrafish embryos, indicating that these factors are sufficient to specify endothelial fate

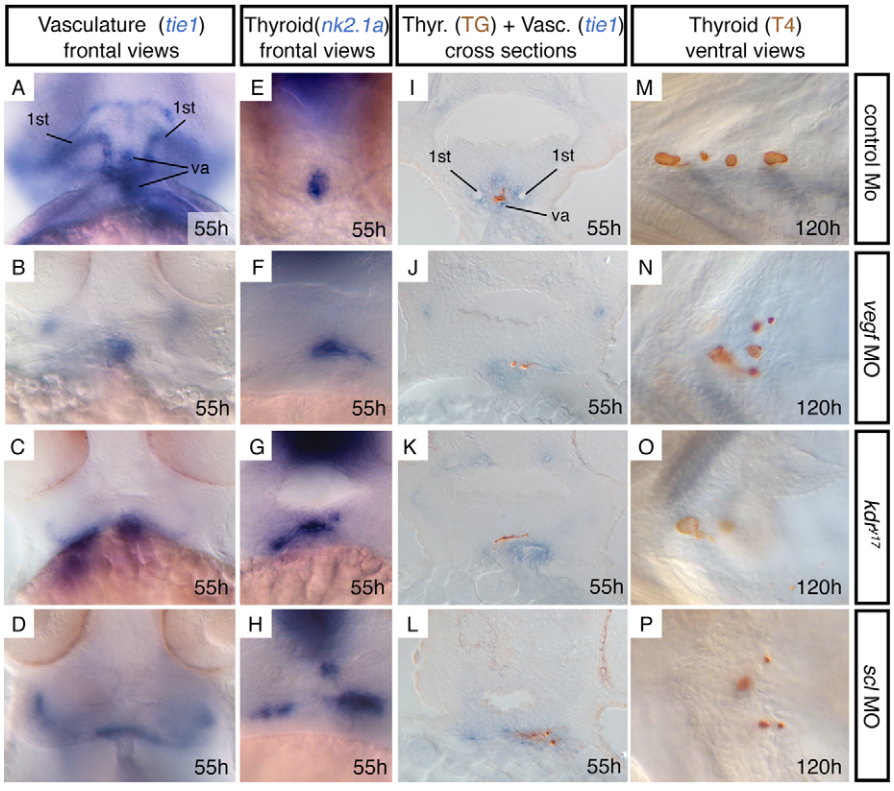

Fig. 2. Mutants with defects in ventral aorta development show correlating thyroid abnormalities. (**A-H**) Frontal views, showing vasculature (*tie1* expression) or thyroid (*nk2.1a* expression). Control morpholino injected embryos are indistinguishable from wild-type embryos or kdr^{y17} siblings. (**I-L**) Sections showing folliclular lumen (thyroglobulin immunostaining, brown) in relation to endothelial cells (*tie1* expression, blue). (**M-P**) At 120 hpf, thyroid follicles (T4 immunostaining, brown) fail to align along the ventral aorta. In F-H,J-L the thyroid appears larger owing to the lateral expansion. However, in wild-type embryos the thyroid extends along the AP axis (compare with Fig. 1B). Concomitant with lateral expansion, its AP extent appears to be reduced, so that the size remains similar. This is also reflected by normal follicle numbers at 120 hpf (M-P). TG, thyroglobulin; Thyr, thyroid; Vasc, vasculature; va, ventral aorta; 1st, first pair of branchial arteries.

in all head mesenchymal cells (Gering et al., 2003). Similarly, co-injection of these mRNAs induces strong *kdr* expression in the whole head mesenchyme (Fig. 3A-D). Such injected embryos develop extreme head abnormalities and die around 24 hpf (data not shown), preventing the analysis of thyroid development. Instead, we grafted cells from *scl+lmo2* co-injected embryos into wild-type hosts in order to create a mosaic of wild-type and ectopic endothelial cells.

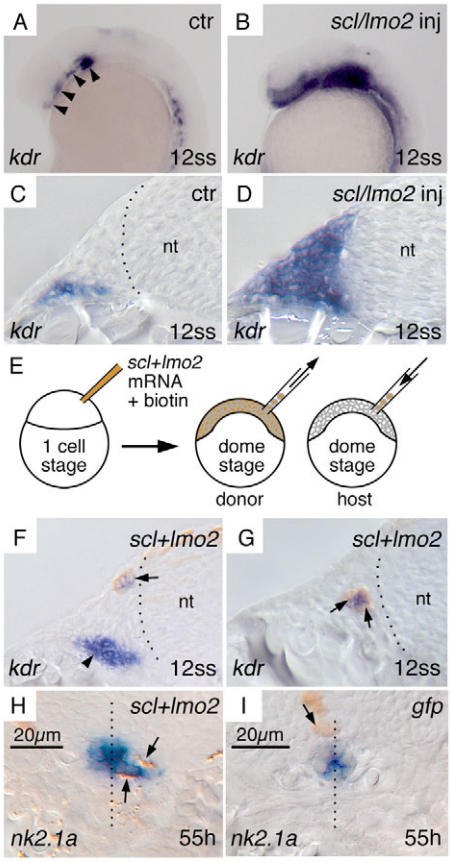

Fig. 3. Ectopic endothelial cells can influence thyroid morphology cell non-autonomously. Lateral views (A,B) and cross-sections (C-I) through the head region. (**A**,**C**) In wild-type embryos, bilateral groups of *kdr* domains (arrowheads) mark part of the anterior (head) lateral plate mesoderm that give rise to vascular structures. (**B**,**D**) Co-injection of *scl* and *lmo2* mRNA leads to massive upregulation of *kdr* in the head mesenchyme of zebrafish embryos. (**E**) Experimental procedure: donor cells from *scl* and *lmo2* co-injected embryos were grafted into wild-type embryos. (**F**,**G**) Donor cells have all developed into endothelial cells when found in the head mesenchyme of host embryos. Arrows indicate *kdr* expression (blue) overlapping with the cell marker biotin (brown) present in grafted cells. Endogenous *kdr* expression (arrowhead in F) is variably visible on sections, depending on the exact level of sectioning (compare with A). (**H**) At 55 hpf, grafted *scl+lmo2* cells (brown, arrows) have caused the thyroid primordium (blue) to expand laterally. One of the four embryos where grafted cells were detected adjacent to the thyroid primordium. (**I**) An embryo where *gfp* injected donor cells are found close to the thyroid, which is not expanded towards the grafted cell. In H and I, care was taken to chose the section through the median level of the thyroid, and diameters were measured on the base of these sections. In I, nuclei in the thyroid appear more prominent than in H, so that the cytoplasmic *nk2.1a* signal looks slightly weaker on this median section. Broken lines indicate the border of the neural tube (nt) in C,F,G, and the midline in H,I. 12 ss, 12 somite stage.

In this transplantation approach, few cells were grafted at late blastula stage from *scl+lmo2* mRNA injected donors into wild-type hosts (Fig. 3E). We analysed some embryos at 12-somite stage, when head vasculogenesis is in progress (Gering et al., 2003), and ectopic endothelial cells can easily be distinguished from normal sites of expression. In all embryos investigated, all grafted cells ending up in head mesenchyme express *kdr*, and, hence, adopt endothelial fate (12 of 12 sectioned embryos; Fig. 3F,G).

For analysis of thyroid development, we fixed other host embryos at 55 hpf. In most of these embryos, the thyroid appears normal, even if grafted cells are found in the pharyngeal region (n=14). However, exclusively in four embryos where grafted cells ended up directly adjacent to the medially positioned thyroid, its tissue projects towards the grafted cells (Fig. 3H). In all four cases, the thyroid marker *nk2.1* itself is not expressed in the grafted cells. As a control, we grafted cells from *gfp* mRNA-injected embryos into wild-type embryos. Out of 28 embryos that received grafted *gfp* cells, seven had donor cells very close to the thyroid. All of these embryos, as well as all other embryos where *gfp* or *scl+lmo2* donor cells were further away from the thyroid, had a normal gland without projections towards grafted cells (Fig. 3I). To further compare both

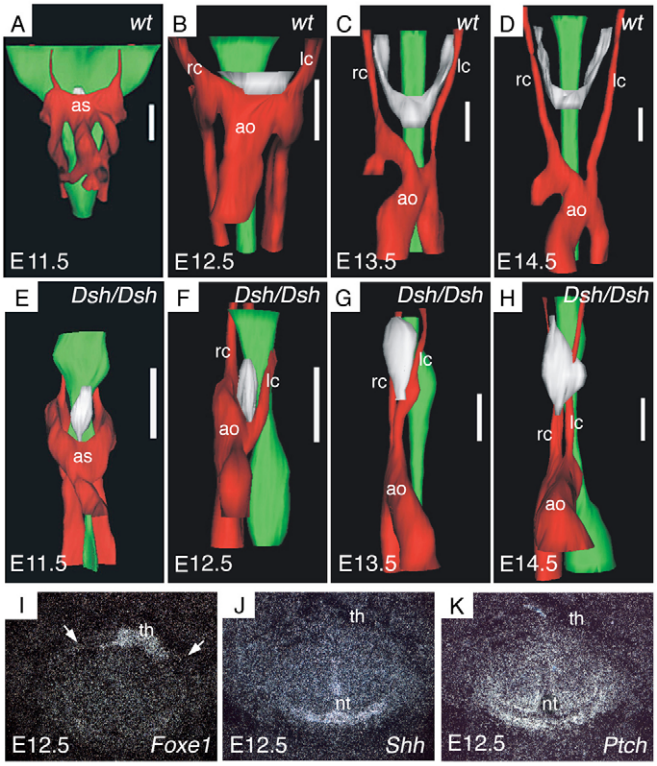

Fig. 4. Thyroid morphogenesis is disturbed in *short digits* (*Dsh/Dsh*) mutant mice. (**A-D**) Three-dimensional reconstruction of the cervical region in wild-type mice. (**E-H**) Same reconstruction of *Dsh/Dsh* mutant mice. Stages are indicated in the bottom left-hand corner. Red, vascular structures; green, oesophagus; white, thyroid primordium. Scale bar: 140 μm. (**I-K**) Expression of sonic hedgehog (J) and patched (K) in wild-type E12.5 mouse embryos. Consecutive sections processed for in situ hybridisation, in comparison with the thyroid marker *Foxe1* (I). *Shh* and *Ptch* are expressed in or around the neural tube, but not in the area of the thyroid. White arrows indicate the position of the carotid arteries (visible in corresponding bright field views). ao, aortic arch; as, aortic sac; lc, left carotid artery; nt, neural tube; rc, right carotid artery; th, thyroid.

Table 1. Neighbouring *scl+lmo2*-expressing cells change the shape of the wild-type thyroid

Grafted specimen (lab code)	Width	Length	Width/Length
gfp-25	12.4	15.6	0.79
gfp-14	11.7	15.5	0.75
gfp-4	12.2	16.7	0.73
gfp-2	10.8	15.7	0.69
gfp-18	13.8	14.5	0.95
gfp-3	13.3	16.1	0.83
gfp-5	13.7	15.4	0.89
Mean value (embryos that received *gfp* grafted cells)	12.6	15.6	0.83
scl+lmo2-4	10.7	29.6	0.36
scl+lmo2-6	15.4	36.1	0.43
scl+lmo2-3	10.2	31.9	0.32
scl+lmo2-8	13.5	24.4	0.55
Mean value (embryos that received *scl+lmo2* grafted cells)	12.5	30.5	0.42

The width and the length (in μm) of the thyroid at 55 hpf are given, as measured on the median thyroid level on cross-sections. Data for the four embryos where *scl+lmo2*-overexpressing cells were found close to the thyroid (lab code: *scl+lmo2*-#), and for seven embryos where control *gfp*-overexpressing cells were found similarly close to the thyroid (lab code: *gfp*-#).

sets of grafting experiments, we measured the width and the length (the smallest and the largest diameter) of the thyroid on its median level in sections. In the seven hosts with *gfp* cells close to the thyroid, the gland generally adopts the normal slightly ovoid shape in cross-sections, with the quotient of both values being around 0.8 (Table 1). In the four hosts with *scl+lmo2* cells close to the thyroid, the abnormally elongated shapes of the gland result in a quotient of only around 0.4 (Table 1). Statistical analysis of the quotient values of all 11 specimens (U-test according to Mann, Wilcoxon, and Whitney) reveals that the thyroid glands of embryos with *scl+lmo2* cells are significantly different from embryos with *gfp* cells (P=0.02). We have shown above that grafted cells in the head mesenchyme behave as endothelial cells. Our grafting experiments show that such cells are able to influence thyroid morphology in a non-cell-autonomous manner in zebrafish.

Together, our zebrafish data indicate that vascular cells influence thyroid morphology. Under wild-type conditions, the ventral aorta is the only vessel adjacent to the thyroid in zebrafish embryos/larvae. Based on both mutant analysis and grafting experiments, we conclude that the ventral aorta acts as an instructive structure for positioning thyroid tissue along the AP axis.

Three-dimensional analysis of wild-type and mutant mouse embryos suggest an influence of carotid arteries on thyroid morphogenesis

A role of the vascular system in thyroid development has been suspected in mice based on the close spatial relationship between aortic sac and thyroid primordium. However, these studies focused on an hypothetical early role of the aortic sac in induction and evagination of the primordium (Fagman et al., 2005). To test whether an instructive role of blood vessels in subsequent steps of thyroid morphogenesis could be conserved among vertebrates, we analysed three-dimensional reconstruction of cervical regions of wild-type and mutant mouse embryos. Thyroid precursor cells firstly occur within the pharyngeal epithelium in direct contact to the aortic sac (Fig. 4A), a transient structure that gives rise to the cardiac outflow tract. Under wild-type conditions, the primordium first relocates along the AP axis in close contact to the developing aortic arch (Fig. 4B). Later, the primordium loses its contact to the aortic arch and bifurcates (Fig. 4C). During bifurcation the thyroid lobes are again close to vascular structures, the bilateral pair of carotid arteries. Subsequently, the lobes elongate following the carotid arteries further cranially (Fig. 4D). We therefore asked whether carotid arteries play a similar role in mammalian thyroid morphology as the ventral aorta does in zebrafish.

Recent work has shown that an abnormal, unilateral single thyroid lobe develops in *Shh*-deficient mouse embryos (Fagman et al., 2004). Furthermore, *Shh* deficiency leads to defective cardiac rotation and atrial dilatation (Tsukui et al., 1999), suggesting further defects in cervical vessel development. Three dimensional reconstruction of sections reveals that in the absence of *Shh* expression (in *Dsh/Dsh* mice) (Niedermaier et al., 2005), the aortic arch fails to cross the midline and both carotid arteries develop asymmetrically on one side of the oesophagus (Fig. 4E-H). Initially, the thyroid primordium evaginates and relocates along the AP axis in the midline of *Shh*-deficient mice as in wild type (Fig. 4E). However, the primordium then fails to undergo its symmetric lateralisation and bifurcation. Instead, after embryonic day 12.5, a single lobe always relocates on the same side as and in contact with the mislocated carotid arteries (right n=7, left n=1; Fig. 4F-H, Fig. 5D), suggesting that the carotid arteries define the symmetric lateral position of the thyroid gland under wild-type conditions.

Compromised hedgehog signalling affects many aspects of embryonic development, and so it could be that thyroid and vessels are independently affected in *Dsh/Dsh* mice. However, we did not find detectable expression of *Shh* or patched (encoding the receptor for Shh) in or around carotid arteries or the thyroid primordium at E12.5, when asymmetry of thyroid and carotid arteries starts to be evident in Dsh/Dsh mice (Fig. 4I-K). Although we cannot exclude low levels of expression, it appears unlikely that Shh is directly involved in thyroid relocalisation at this stage. Instead, it is more likely that Shh deficiency causes vascular problems that indirectly affect thyroid morphology.

Furthermore, we investigated thyroid and carotid artery morphology in a mutant background where the *Dsh/Dsh* phenotype is partially restored to wild-type appearance. *Shh* and *Gli3* are context-dependent antagonists of each other in mouse limb and neural tube development, so that in $Shh^{-/-}$ $Gli3^{-/-}$ double mutants, some aspects of the $Shh^{-/-}$ mutant phenotype are rescued (Ruiz i Altaba et al., 2003; te Welscher et al., 2002). We found that in this double mutant background (*Dsh/Dsh* Xt^J/Xt^J, Xt^J is a null allele of

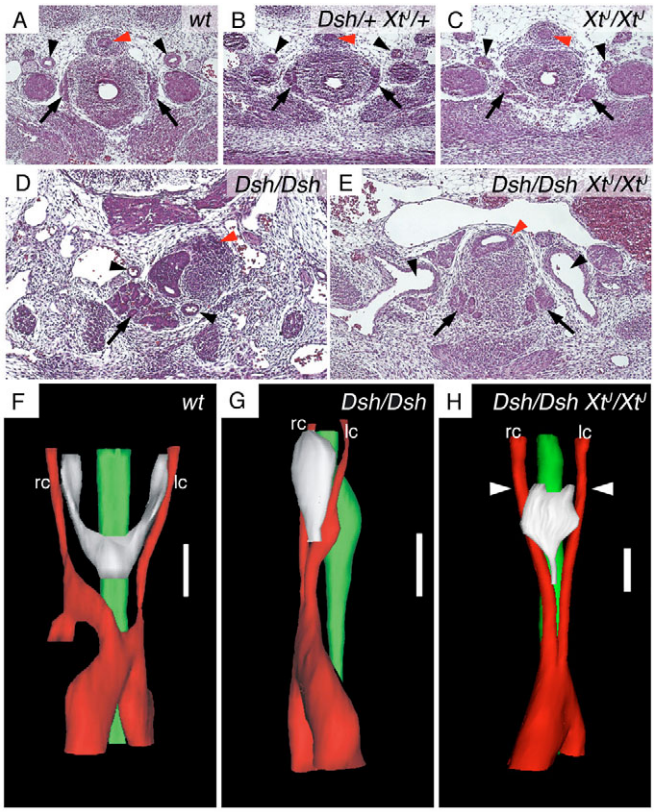

Fig. 5. In *Dsh/Dsh Xt^J/Xt^J* double mutants, symmetry of carotid arteries is restored and the thyroid primordium regains its midline position. HE staining of representative histological sections (A-E) and three-dimensional reconstruction (F-H) of E13.5 mouse embryos. (**A-C**) Both carotid arteries (arrowheads) and thyroid lobes (arrows) are normal in double heterozygous or *Xt^J/Xt^J* mouse embryos. (**D**,**E**) Whereas in *Dsh/Dsh* mice both carotid arteries and mis-shaped thyroid are positioned unilaterally (D), a bilateral set of carotid arteries (arrowheads) forms in double homozygous *Dsh/Dsh Xt^J/Xt^J* mice (E), and the thyroid develops into a bilateral set of lobes at its cranial end (arrows). The carotid arteries in E are larger than in wild type but their identity is unequivocally due to their arterial walls and origin from the aortic arch (as revealed by series of sections, data not shown). Red arrowheads indicate the oesophagus. A-E are at the same magnification; D,E show larger areas. (**F-H**) Three-dimensional reconstruction visualising how the carotid arteries and the thyroid have regained bilateral positions in *Dsh/Dsh Xt^J/Xt^J* mice. White arrowheads indicate the level of the section in E, showing the symmetrical cranial lobes of the thyroid. The thyroid is still abnormally shaped, probably owing to the close distance between the carotid arteries. lc, left carotid artery; rc, right carotid artery. Scale bars: 140 μm.

Gli3) (Persson et al., 2002), the bilateral set of carotid arteries is restored to its symmetrical appearance and the thyroid regains a midline position with symmetrical, bilateral cranial lobes (n=3) (Fig. 5). This parallel restoration of symmetry further demonstrates the close co-development of both structures. Owing to a lack of mouse mutants with more specific defects in carotid artery development, a direct interaction between these vessels and the thyroid has still to be shown for mice. However, in the light of the zebrafish data it is likely that in mice vascular and thyroid development are also functionally linked, and that dependence of thyroid tissue localisation on co-developing arteries is a conserved mechanism in vertebrates.

DISCUSSION

The thyroid gland in vertebrates develops close to vascular structures. In the present study, we analyse zebrafish and mouse embryos with altered vessel architecture and find that defects in pharyngeal/cervical vessels coincide with abnormal thyroid development in both species. The study of zebrafish embryos with ectopic endothelial cells reveals a functional link between vascular and thyroid development.

Our zebrafish data show that ectopic endothelial cells influence thyroid morphology in a non-cell autonomous manner. In mice, vessels are involved in induction of the endoderm-derived pancreas from the primitive gut (Lammert et al., 2001). A role of the cardiovascular system in induction of the mouse thyroid has been suspected (Fagman et al., 2005), and so ectopic induction could probably also cause lateral expansion of thyroid tissue in the zebrafish embryos lacking Scl or with compromised Vegf signalling. However, as reported above, in all deficiency backgrounds analysed, the thyroid starts to develop from a normally induced midline primordium. Therefore, an inductive role of vascular structures can be excluded to be responsible for the thyroid phenotypes observed in our deficiency backgrounds. Furthermore, in *cloche*, a zebrafish mutant lacking all vessel progenitors in head and anterior trunk region (Liao et al., 1997; Stainier et al., 1995), the thyroid primordium is still induced (data not shown). As the myocard forms in *cloche*, it is still possible that the heart or some of its precursor cells are involved in thyroid induction, but an inductive role of vessels can be excluded.

Cell labelling experiments suggest that the whole strand of thyroid tissue in zebrafish derives from the small globular primordium that buds off from the pharyngeal epithelium at around 32 hpf (Alt et al., 2006), and that no further cells contribute to the thyroid from outside during its extension along the AP axis. This, and the fact that in our deficiency backgrounds the thyroid primordium is initially normal, suggest that in our grafting experiments the lateral expansion of thyroid tissue adjacent to endothelial cells is generated by misdirected growth. Taken together, our zebrafish data show that endothelial cells are required for proper alignment of thyroid tissue along the AP axis during tissue growth.

The grafting experiments show an instructive influence of endothelial cells on thyroid morphogenesis, but we were not able to discriminate between different endothelial cell types in this experiment. Under wild-type conditions, the ventral aorta is the only vessel directly adjacent to the thyroid in zebrafish, so that it can be assumed that this is the vessel responsible for interactions with the thyroid. Not only in zebrafish (Wendl et al., 2002), but also in other teleosts such as trouts (Raine and Leatherland, 2000), thyroid tissue remains in close association with the ventral aorta throughout later development and adulthood. It will be interesting to find out how such an interaction is mediated. Extracellular matrix or secreted factors are candidates, but the exact nature of the interaction between vessels and thyroid tissue remains to be elucidated.

In both zebrafish and mouse development, two morphogenetic phases are distinguishable in thyroid relocalisation. After induction and evagination, the thyroid primordium adopts a position close to the cardiac outflow tract in zebrafish or to the aortic sac in mice, respectively (Fig. 6). In all deficiency backgrounds investigated, this first phase is not disrupted. Consequently, follicles cluster at a default position around the cardiac outflow tract in the deficient zebrafish larvae, and the primordium initially relocalises correctly in the midline of E11.5 *Dsh/Dsh* mice. In a second phase of relocalisation that is dependent on ventral aorta or carotid artery development, the thyroid then adopts its species-specific position

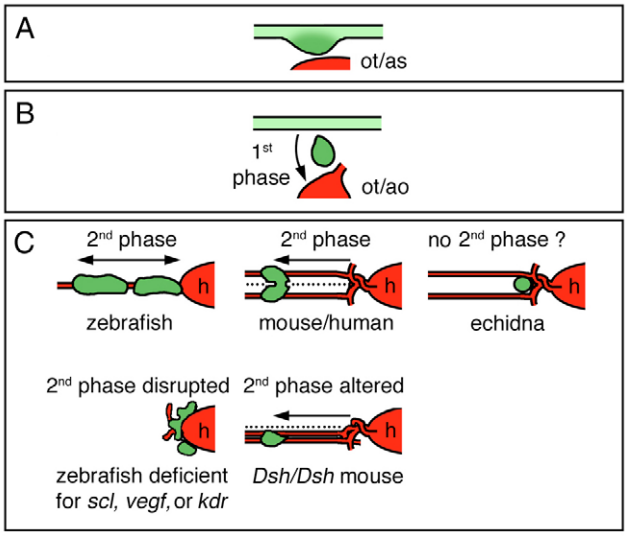

Fig. 6. Thyroid relocalisation in vertebrates involves two morphogenetic phases. Schematic drawing summarising morphogenetic aspects in thyroid development of vertebrates. (A-C) Selected stages of thyroid development. Red, cardiovascular system; light green, pharyngeal epithelium; dark green, thyroid tissue. Cranial is towards the left. A and B are lateral views, schematics in C are dorsal or ventral views. (**A**) Evagination of the primordium from the pharyngeal epithelium on the level of the outflow tract of the heart in zebrafish or the aortic sac in mice, respectively. (**B**) First phase of relocalisation, visualised by the black arrow, close to the outflow tract or the aortic arch. (**C**) Distribution of thyroid tissue in larval stages (zebrafish), late embryonic stages (mouse) or adult (echidna). A second phase of relocalisation as shown for zebrafish and mouse is indicated by arrows. The directionality of growth of thyroid tissue in zebrafish is uncertain (bi-directional arrow), as ventral aorta and thyroid grow concomitantly. In the adult echidna, the thyroid is positioned at the base of the cervical arteries. Despite a lack of embryological data, it is tempting to assume that in this species a second phase of morphogenetic changes is reduced or missing. The midline is indicated by broken lines. ao, aortic arch; as, aortic sac; ot, outflow tract.

further cranially. In the complex and derived circulation of mice, the aortic sac is in part homologous to the cardiac outflow tract and probably also to the ventral aorta in zebrafish. Thus, the first phase of thyroid relocalisation from the pharyngeal epithelium to cardiac structures appears to be evolutionary conserved, whereas the second phase seems to be adapted to the presence of different cranial vessels.

These data suggest that the dependence of thyroid morphogenesis on the development of adjacent arteries is a conserved mechanism that might have evolved to ensure efficient hormone release into circulation. Interestingly, the identity of vessels with instructive influence on thyroid localisation appears to vary considerably in vertebrates. In most vertebrates, two thyroid lobes are positioned cranial to the aortic arch, midway along the carotid arteries, as is the case in mice and humans (Pischinger, 1937). Conversely, in some vertebrates such as crocodiles, turtles, and certain mammals as the echidna (Haynes, 1999; Pischinger, 1937), a single-lobed thyroid is positioned further caudally at the aortic arch, at the base of the branching carotid arteries (Fig. 6). Thus, it appears that the second morphogenetic phase is omitted in these species.

Our data provide a novel starting point to re-investigate and interpret congenital thyroid defects in humans. Cervical vessel architecture is highly variable in humans, in particular with respect to the branching mode of the carotid arteries from the aortic arch that can be classified into few frequent and many rare variants (Nizankowski et al., 1975). Based on our data, it is conceivable that some variants might influence thyroid morphogenesis and account for cases of unilateral thyroid glands or ectopically positioned thyroid tissue in humans. Indeed, in clinical studies, congenital defects of the cardiovascular system have already been associated with congenital thyroid abnormalities (Casanova et al., 2000; Olivieri et al., 2002), and our study is the first to provide a causal link between both structures in development. Thus, the disruption of signalling pathways linking thyroid and blood vessel development represents a novel mechanism that is likely to be relevant for the molecular pathogenesis of congenital thyroid defects in humans.

We thank Julia von Gartzen and Frank van Landegem for excellent technical assistance; Andrea Vortkamp and Uli Rüther for supplying the *Xt*^{J} mice; and Stephen Wilson, Heike Biebermann and Martin Gering for critical comments on the manuscript, support and discussion. We are grateful to Alexandra Franzmann for help and advice on statistical analysis. B.A. and K.B.R. are supported by DFG: SFB 572; H.K. by BMBF-NBL3 and DFG: SFB 577; and O.A.E. by Garyounis University (Libya).

References

Alt, B., Reibe, S., Feitosa, N. M., Elsalini, O. A., Wendl, T. and Rohr, K. B. (2006). Analysis of origin and growth of the thyroid gland in zebrafish. *Dev. Dyn.* **235**, 1872-1883.

Casanova, J. B., Daly, R. C., Edwards, B. S., Tazelaar, H. D. and Thompson, G. B. (2000). Intracardiac ectopic thyroid. *Ann. Thorac. Surg.* **70**, 1694-1696.

Castanet, M., Park, S. M., Smith, A., Bost, M., Leger, J., Lyonnet, S., Pelet, A., Czernichow, P., Chatterjee, K. and Polak, M. (2002). A novel loss-of-function mutation in TTF-2 is associated with congenital hypothyroidism, thyroid agenesis and cleft palate. *Hum. Mol. Genet.* **11**, 2051-2059.

Covassin, L. D., Villefranc, J. A., Kacergis, M. C., Weinstein, B. M. and Lawson, N. D. (2006). Distinct genetic interactions between multiple Vegf receptors are required for development of different blood vessel types in zebrafish. *Proc. Natl. Acad. Sci. USA* **103**, 6554-6559.

Dathan, N., Parlato, R., Rosica, A., De Felice, M. and Di Lauro, R. (2002). Distribution of the titf2/foxe1 gene product is consistent with an important role in the development of foregut endoderm, palate, and hair. *Dev. Dyn.* **224**, 450-456.

De Felice, M. and Di Lauro, R. (2004). Thyroid development and its disorders: genetics and molecular mechanisms. *Endocr. Rev.* **25**, 722-746.

Elsalini, O. A. and Rohr, K. B. (2003). Phenylthiourea disrupts thyroid function in developing zebrafish. *Dev. Genes Evol.* **212**, 593-598.

Elsalini, O. A., von Gartzen, J., Cramer, M. and Rohr, K. R. (2003). Zebrafish hhex, nk2.1a and pax2.1 regulate thyroid growth and differentiation downstream of Nodal-dependent transcription factors. *Dev. Biol.* **263**, 67-80.

Fagman, H., Grande, M., Gritli-Linde, A. and Nilsson, M. (2004). Genetic deletion of sonic hedgehog causes hemiagenesis and ectopic development of the thyroid in mouse. *Am. J. Pathol.* **164**, 1865-1872.

Fagman, H., Andersson, L. and Nilsson, M. (2005). The developing mouse thyroid: embryonic vessel contacts and parenchymal growth pattern during specification, budding, migration, and lobulation. *Dev. Dyn.* **235**, 444-445.

Ferrara, N. (2004). Vascular endothelial growth factor: basic science and clinical progress. *Endocr. Rev.* **25**, 581-611.

Gering, M., Rodaway, A. R., Gottgens, B., Patient, R. K. and Green, A. R. (1998). The SCL gene specifies haemangioblast development from early mesoderm. *EMBO J.* **17**, 4029-4045.

Gering, M., Yamada, Y., Rabbitts, T. H. and Patient, R. K. (2003). Lmo2 and Scl/Tal1 convert non-axial mesoderm into haemangioblasts which differentiate into endothelial cells in the absence of Gata1. *Development* **130**, 6187-6199.

Gorbman, A. and Bern, H. A. (1962). *Textbook of Comparative Endocrinology*. New York: John Wiley.

Habeck, H., Odenthal, J., Walderich, B., Maischein, H., Schulte-Merker, S. and Tubingen 2000 screen consortium (2002). Analysis of a zebrafish VEGF receptor mutant reveals specific disruption of angiogenesis. *Curr. Biol.* **12**, 1405-1412.

Haynes, J. I. (1999). Parathyroids and ultimobranchial bodies in monotremes. *Anat. Rec.* **254**, 269-280.

Isogai, S., Horiguchi, M. and Weinstein, B. M. (2001). The vascular anatomy of the developing zebrafish: an atlas of embryonic and early larval development. *Dev. Biol.* **230**, 278-301.

Jin, H., Xu, J., Qian, F., Du, L., Tan, C. Y., Lin, Z., Peng, J. and Wen, Z. (2006). The 5′ zebrafish scl promoter targets transcription to the brain, spinal cord, and hematopoietic and endothelial progenitors. *Dev. Dyn.* **235**, 60-67.

Lammert, E., Cleaver, O. and Melton, D. (2001). Induction of pancreatic differentiation by signals from blood vessels. *Science* **294**, 564-567.
Lawson, N. D., Vogel, A. M. and Weinstein, B. M. (2002). sonic hedgehog and vascular endothelial growth factor act upstream of the Notch pathway during arterial endothelial differentiation. *Dev. Cell* **3**, 127-136.
Liao, E. C., Paw, B. H., Oates, A. C., Pratt, S. J., Postlethwait, J. H. and Zon, L. I. (1998). SCL/Tal-1 transcription factor acts downstream of cloche to specify hematopoietic and vascular progenitors in zebrafish. *Genes Dev.* **12**, 621-626.
Liao, W., Bisgrove, B. W., Sawyer, H., Hug, B., Bell, B., Peters, K., Grunwald, D. J. and Stainier, D. Y. (1997). The zebrafish gene cloche acts upstream of a flk-1 homologue to regulate endothelial cell differentiation. *Development* **124**, 381-389.
Maiorana, R., Carta, A., Floriddia, G., Leonardi, D., Buscema, M., Sava, L., Calaciura, F. and Vigneri, R. (2003). Thyroid hemiagenesis: prevalence in normal children and effect on thyroid function. *J. Clin. Endocrinol. Metab.* **88**, 1534-1536.
Nasevicius, A., Larson, J. and Ekker, S. C. (2000). Distinct requirements for zebrafish angiogenesis revealed by a VEGF-A morphant. *Yeast* **17**, 294-301.
Niedermaier, M., Schwabe, G. C., Fees, S., Helmrich, A., Brieske, N., Seemann, P., Hecht, J., Seitz, V., Stricker, S., Leschik, G. et al. (2005). An inversion involving the mouse Shh locus results in brachydactyly through dysregulation of Shh expression. *J. Clin. Invest.* **115**, 900-909.
Nizankowski, C., Rajchel, Z. and Ziolkowski, M. (1975). Abnormal origin of arteries from the aortic arch in man. *Folia Morphol. Warsz.* **34**, 109-116.
Olivieri, A., Stazi, M. A., Mastroiacovo, P., Fazzini, C., Medda, E., Spagnolo, A., De Angelis, S., Grandolfo, M. E., Taruscio, D., Cordeddu, V. et al. (2002). A population-based study on the frequency of additional congenital malformations in infants with congenital hypothyroidism: data from the Italian Registry for Congenital Hypothyroidism (1991-1998). *J. Clin. Endocrinol. Metab.* **87**, 557-562.
Patterson, L. J., Gering, M. and Patient, R. (2005). Scl is required for dorsal aorta as well as blood formation in zebrafish embryos. *Blood* **105**, 3502-3511.
Persson, M., Stamataki, D., te Welscher, P., Andersson, E., Bose, J., Ruther, U., Ericson, J. and Briscoe, J. (2002). Dorsal-ventral patterning of the spinal cord requires Gli3 transcriptional repressor activity. *Genes Dev.* **16**, 2865-2878.
Pischinger, P. (1937). Kiemenanlagen und ihre Schicksale bei Amnioten. Schilddrüse und epitheliale Organe der Pharynxwand bei Tetrapoden. In *Handbuch der Vergleichenden Anatomie der Wirbeltiere*. Vol. 3 (ed. L. Bolk, E. Göppert, E. Kallius and W. Lubosch), pp. 279-348. Berlin, Wien: Urban and Schwarzenberg.
Raine, J. C. and Leatherland, J. F. (2000). Morphological and functional development of the thyroid tissue in rainbow trout (Oncorhynchus mykiss) embryos. *Cell Tissue Res.* **301**, 235-244.
Rohr, K. B. and Concha, M. L. (2000). Expression of nk2.1a during early development of the thyroid gland in zebrafish. *Mech. Dev.* **95**, 267-270.
Ruiz i Altaba, A., Nguyen, V. and Palma, V. (2003). The emergent design of the neural tube: prepattern, SHH morphogen and GLI code. *Curr. Opin. Genet. Dev.* **13**, 513-521.
Sehnert, A. J., Huq, A., Weinstein, B. M., Walker, C., Fishman, M. and Stainier, D. Y. (2002). Cardiac troponin T is essential in sarcomere assembly and cardiac contractility. *Nat. Genet.* **31**, 106-110.
Stainier, D. Y., Weinstein, B. M., Detrich, H. W., 3rd, Zon, L. I. and Fishman, M. C. (1995). Cloche, an early acting zebrafish gene, is required by both the endothelial and hematopoietic lineages. *Development* **121**, 3141-3150.
te Welscher, P., Zuniga, A., Kuijper, S., Drenth, T., Goedemans, H. J., Meijlink, F. and Zeller, R. (2002). Progression of vertebrate limb development through SHH-mediated counteraction of GLI3. *Science* **298**, 827-830.
Tsukui, T., Capdevila, J., Tamura, K., Ruiz-Lozano, P., Rodriguez-Esteban, C., Yonei-Tamura, S., Magallon, J., Chandraratna, R. A., Chien, K., Blumberg, B. et al. (1999). Multiple left-right asymmetry defects in Shh(–/–) mutant mice unveil a convergence of the shh and retinoic acid pathways in the control of Lefty-1. *Proc. Natl. Acad. Sci. USA* **96**, 11376-11381.
Wendl, T., Lun, K., Mione, M., Favor, J., Brand, M., Wilson, S. W. and Rohr, K. B. (2002). pax2.1 is required for the development of thyroid follicles in zebrafish. *Development* **129**, 3751-3760.
Yamada, Y., Warren, A. J., Dobson, C., Forster, A., Pannell, R. and Rabbitts, T. H. (1998). The T cell leukemia LIM protein Lmo2 is necessary for adult mouse hematopoiesis. *Proc. Natl. Acad. Sci. USA* **95**, 3890-3895.
Yamada, Y., Pannell, R., Forster, A. and Rabbitts, T. H. (2000). The oncogenic LIM-only transcription factor Lmo2 regulates angiogenesis but not vasculogenesis in mice. *Proc. Natl. Acad. Sci. USA* **97**, 320-324.